Physics and Imaging in Radiation Oncology 17 (2021) 71–76

Contents lists available at ScienceDirect

Physics and Imaging in Radiation Oncology

journal homepage: www.sciencedirect.com/journal/physics-and-imaging-in-radiation-oncology

Original Research Article

Cone beam computed tomography for dose calculation quality assurance for magnetic resonance-only radiotherapy

Jonathan J. Wyatt [a,b,*], Rachel A. Pearson [a,b], Christopher P. Walker [a], Rachel L. Brooks [a], Karen Pilling [a], Hazel M. McCallum [a,b]

[a] Northern Centre for Cancer Care, Newcastle upon Tyne Hospitals NHS Foundation Trust, Newcastle, UK
[b] Centre for Cancer, Newcastle University, Newcastle, UK

ARTICLE INFO

Keywords:
MR-only radiotherapy planning
Magnetic resonance imaging
Radiotherapy
Prostate cancer
Cone beam computed tomography
Image guided radiation therapy
Quality assurance

ABSTRACT

Background and purpose: Magnetic Resonance (MR)-only prostate radiotherapy using synthetic Computed Tomography (sCT) algorithms with high dose accuracy has been clinically implemented. MR images can suffer from geometric distortions so Quality Assurance (QA) using an independent, geometrically accurate, image could be required. The first-fraction Cone Beam CT (CBCT) has demonstrated potential but has not been evaluated in a clinical MR-only pathway. This study evaluated the clinical use of CBCT for dose accuracy QA of MR-only radiotherapy.

Materials and methods: A total of 49 patients treated with MR-only prostate radiotherapy were divided into two cohorts. Cohort 1 (20 patients) received a back-up CT, whilst Cohort 2 (29 patients) did not. All patients were planned using the sCT and received daily CBCT imaging with MR-CBCT soft-tissue matching. Each CBCT was calibrated using a patient-specific stepwise Hounsfield Units-to-mass density curve. The treatment plan was recalculated on the first-fraction CBCT using the clinically applied soft-tissue match and the doses compared. For Cohort 1 the sCT was rigidly registered to the back-up CT, the plan recalculated and doses compared.

Results: Mean sCT-CBCT dose difference across both cohorts was $-0.6 \pm 0.1\%$ (standard error of the mean, range $-2.3\%, 2.3\%$), with 47/49 patients within $[-2\%, 1\%]$. The sCT-CBCT dose difference was systematically lower than the sCT-CT by $-0.7 \pm 0.6\%$ ($\pm$95% limits of agreement). The mean sCT-CBCT gamma pass rate (2%/2 mm) was $96.1 \pm 0.4\%$ (85.4%, 99.7%).

Conclusions: CBCT-based dose accuracy QA for MR-only radiotherapy appears clinically feasible. There was a small systematic sCT-CBCT dose difference implying asymmetric tolerances of $[-2\%, 1\%]$ would be appropriate.

1. Introduction

Magnetic Resonance (MR)-only radiotherapy enables the superior soft-tissue contrast of MR [1] to be used for organ delineation without the uncertainty of registering to a Computed Tomography (CT) image [2]. MR-only radiotherapy requires a method of generating a synthetic CT (sCT) from the MR that can be used for radiotherapy dose calculations [3]. This has been the focus of significant research effort in recent years and commercially available solutions are now being used clinically in the treatment of prostate cancer [4,5].

These sCT algorithms have demonstrated high dose calculation accuracy [6,7], yet there may be situations where they fail to generate accurate tissue densities. These situations include artefacts in the MR image, particularly those that affect the patient external contour such as motion and phase wrap artefacts, and for atlas-based algorithms patients substantially larger than the atlas patients [8]. In addition, MR images can suffer from geometric distortion [9], which can vary depending on the patient and scanning parameters [10]. Dose accuracy depends on both the correct assignment of tissue densities and the geometric accuracy of the image. The magnitude of the error introduced would be very variable, but in principle could be clinically significant. For example, failure to apply vendor 3D geometric distortion can increase geometric distortions at the patient external contour from < 2 mm to nearly 8 mm [11], which could produce a dose difference of ~4% in a 6 MV beam. Dose uncertainties of this magnitude would be more problematic than the removal of the 2 mm MR-to-CT registration uncertainty [2] that MR-only enables.

This means ongoing Quality Assurance (QA) of sCT dose calculation

* Corresponding author.
E-mail address: jonathanwyatt@nhs.net (J.J. Wyatt).

https://doi.org/10.1016/j.phro.2021.01.005
Received 3 July 2020; Received in revised form 19 January 2021; Accepted 20 January 2021
Available online 2 February 2021

accuracy is important for MR-only pathways [12]. The standard method for evaluating the dose accuracy of sCTs has been recalculating radiotherapy treatment plans on a CT image of the same patient and comparing the dose distributions. But patients on clinical MR-only pathways will not have CTs and so an alternative methodology needs to be developed for ongoing dose accuracy QA of sCTs.

Independent monitor unit check calculations are a well-established part of the radiotherapy workflow. However, all independent monitor unit check calculations use the patient geometry as defined by the planning image and so will not detect geometric inaccuracies. In addition, algorithms that use the Hounsfield Units (HU) from the planning image will not detect inaccuracies in tissue density assignment in the sCT. Therefore conventional independent monitor unit check methods are not sufficient for ongoing dose accuracy QA of a MR-only pathway.

Edmund et al. proposed using the first-fraction Cone Beam (CB) CT as a QA tool for MR-only radiotherapy [13]. They demonstrated that using a population-based calibration curve gave good agreement between CT and CBCT relative electron densities for six brain patients, suggesting that CBCT could be used to evaluate the dose accuracy of sCT. This methodology was then retrospectively evaluated on 10 prostate patients with sCT-CBCT dose differences agreeing within 1% of gold standard sCT-CT dose differences [14]. The aim of this study was to extend the comparison of sCT-CBCT and sCT-CT dose evaluations and to prospectively evaluate dose accuracy QA using CBCT in a clinical MR-only radiotherapy pathway.

2. Materials and methods

2.1. Patient data collection

A total of 49 patients treated with MR-only radiotherapy for prostate cancer at the Northern Centre for Cancer Care (NCCC), Newcastle upon Tyne, UK were included in this study. The consent for radiotherapy treatment included consent for data to be used for research purposes. Patients were divided into two cohorts: the first 20 patients (Cohort 1) and the remaining 29 patients (Cohort 2). All patients were treated with prostate and seminal vesicle radiotherapy only, with no nodal irradiation.

All patients received a radiotherapy planning MR (1.5 T Magnetom Espree, Siemens, Erlangen, Germany) performed on a flat couch top with local standard prostate radiotherapy immobilisation. Patients in Cohort 1 also received a back-up CT (Sensation Open, Siemens) whereas Cohort 2 patients did not. Prior to each scan and treatment fraction patients underwent routine bladder and bowel preparation, consisting of the application of a micro-enema 60 min prior to the scan, bladder and bowel emptying at 30 min prior and drinking 400 ml of water. The MR images were acquired using a 6 channel flexible receive coil (Siemens Body Matrix) supported over the patient by an in-house manufactured coil bridge and the 24 channel spine receive coil contained in the couch (Siemens Spine Matrix).

The MR images were acquired with a T2-weighted 3D turbo spin echo SPACE (Sampling Perfection with Application optimised Contrasts using different flip angle Evolution) sequence with a field of view of $450 \times 450 \times 180$ mm^3, covering the patient external contour. Geometric distortion was minimised through using a bandwidth of 601 HzPixel^{-1} and applying the Siemens 3D distortion correction algorithm. Measurements with a GRADE phantom (Spectronic Medical, Helsingborg, Sweden) [15] found 99% of phantom markers within the sequence field of view with distortion $D < 2.0$ mm. The sCT images were generated from the MR images using Mriplanner (prostate model version 1.1.7, Spectronic Medical) [16]. The Cohort 1 CT images were acquired with a voxel size of $1.1 \times 1.1 \times 3$ mm^3 and a tube voltage of $V = 120$ kVp.

All patients were planned with a 6 MV single 360^o volumetric modulated arc therapy treatment plan optimised on the sCT delivering a prescription dose of 60 Gy in 20 fractions to 50% of the central Planning Target Volume (PTV) [17] in Raystation (version 7, RaySearch Laboratories, Stockholm, Sweden). A sCT-specific HU to mass density curve provided by Spectronic Medical was used for dose calculations (see Fig. 1). All dose calculations were made with the same beam model using the RayStation collapsed cone algorithm, which calculates dose-to-water. All patients received daily kilovoltage CBCT imaging using a TrueBeam STx (version 2.7 MR3, Varian Medical Systems, Palo Alto, USA), with a voxel size of $0.9 \times 0.9 \times 2$ mm^3, a tube voltage of $V = 125$ kVp and a field of view of 46.5 cm. CBCT images were soft-tissue matched to the planning MR image by treatment radiographers for on-treatment image guidance [18]. This involved an automatic rigid registration between the CBCT and MR images, followed by a manual adjustment to ensure the prostate and seminal vesicles target as visually assessed from the CBCT were included within the PTV delineated on the MR. All patients were then shifted to the soft-tissue match position and treated.

2.2. Dose calculations on CBCT and CT

The first-fraction CBCT was imported in RayStation and registered to the sCT using the online treatment match. The treatment plan was recalculated on the CBCT using the patient-specific step-wise HU to mass density curve available in RayStation. This converted the CBCT image into six tissue classes using patient-specific HU thresholds and assigned

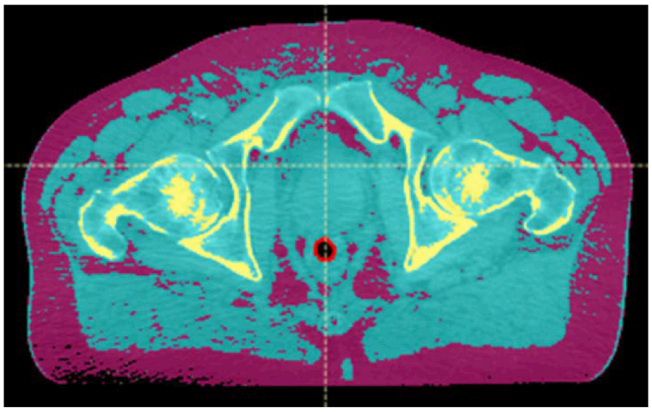

(a) Threshold

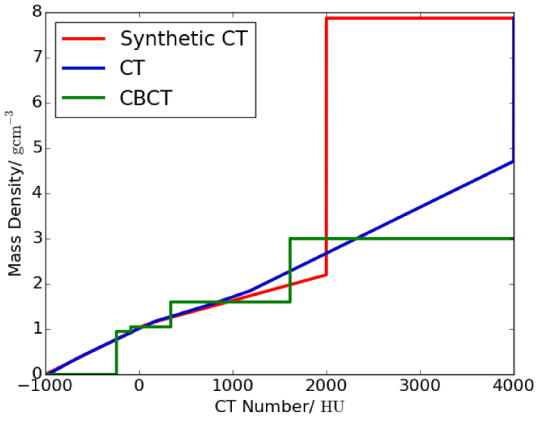

(b) Calibration Curves

Fig. 1. a) Automatic threshold of the CBCT into air (black), adipose (purple), tissue (blue) and cartilage/bone (yellow) (left) and the outlined air in the rectum (red), which was set to $\rho = 1.0$ gcm^{-3}, for a representative patient. b) Plot of CBCT voxel value to mass density curve for the same patient, as well as the Hounsfield Units to mass density curves for the CT and sCT.

the following bulk mass densities: air – 0.00121 gcm^{-3}, lung – 0.26 gcm^{-3}, adipose – 0.95 gcm^{-3}, tissue – 1.05 gcm^{-3}, cartilage/bone - 1.6 gcm^{-3}, and other - 3.0 gcm^{-3} (see example in Fig. 1) [19]. These thresholds were reviewed for each patient and the adipose - tissue threshold manually adjusted in < 10 patients. Dose differences to CT with this method for the pelvis has been reported as $0.2 \pm 1.6\%$ (mean $\pm$ standard deviation) [19]. The body outline on the CBCT was automatically outlined using a RayStation function. Any air in the rectum was outlined and assigned unit density since this process was included in the sCT generation process. The treatment plan was recalculated on the CBCT keeping the monitor units, dose grid voxel size and dose grid position the same.

For the Cohort 1 patients the back-up CT was rigidly registered to the sCT using the automatic mutual information algorithm with six degrees of freedom focused on the PTV in RayStation. A HU to mass density curve derived from data measured on the CT scanner was applied (Fig. 1) and the treatment plan recalculated on the CT with the same monitor units, dose grid voxel size and dose grid position. Any air in the rectum was outlined and assigned unit density.

2.3. Dose evaluation

For both patient cohorts the doses calculated on CBCT and sCT were compared using differences in isocentre dose and a 3D global gamma analysis. The percentage difference in isocentre dose was calculated using

$$\Delta D_{CBCT} = 100\frac{D_{CBCT} - D_{sCT}}{D_{prescription}}, \quad (1)$$

where D_{CBCT} was the dose at the isocentre for the CBCT, D_{sCT} was the dose at the isocentre for the sCT and $D_{prescription}$ the prescription dose. In addition the PTV from the sCT was copied onto the CBCT without modification and the difference in dose to the PTV mean dose, near maximum (D2) and near minimum (D98) were calculated as a percentage of the prescription dose [20].

A gamma analysis was performed comparing the dose calculated on the sCT to the CBCT using the Medical Interactive Creative Environment Toolkit (version 1.0.8, Umea University, Sweden) [21]. Separate gamma analyses were carried out within the external contour and the volume enclosed by the 50% isodose line, using 1% global dose difference of the prescription dose (60 Gy) and 1 mm distance-to-agreement, and 2%/2 mm criteria. All points below 10% of the prescription dose were excluded.

In addition, the 6 MV radiological water equivalent isocentre depth was calculated at 5° angles for each image in the isocentre plane [16,22]. For the CBCT the radiological isocentre depth was calculated using density over-rides for any air in the rectum. For each patient the difference in radiological and physical isocentre depth (CBCT – sCT) at each gantry angle was measured and the mean difference over all gantry angles was calculated. The physical isocentre depth difference was a measure of external contour differences between the images.

For patient Cohort 1, the same dose evaluation methodology was also applied between the sCT and the CT.

2.4. Data analysis

Firstly, Cohort 1 sCT-CT and sCT-CBCT dose differences were compared. Bland–Altman plots of isocentre dose differences and mean physical and radiological isocentre depth differences were generated and the 95% limits of agreement calculated [23].

Secondly, sCT-CBCT data from Cohort 1 was used to generate QA tolerance levels. Only Cohort 1 data was used since the dose accuracy of each patient's sCT had been demonstrated through dose differences with the CT. The 95% confidence interval of the sCT-CBCT isocentre dose difference was calculated and rounded to generate clinical tolerance levels.

Thirdly, sCT-CBCT data from Cohort 2 was evaluated to determine if any patients were outside these tolerance levels, and the cause investigated.

Finally, sCT-CBCT data from cohorts 1 and 2 were evaluated to characterise two factors which might have impacted the results. Firstly, the CBCT dose calculation was carried out at the patient's treated position, a manual adjustment from the optimum MR-CBCT registration (soft-tissue match). To assess the impact of this, the magnitude of the vector shift between the automatic and soft-tissue match positions was calculated for each patient and correlated with the absolute isocentre dose difference. Secondly, the time from MR scan to first-fraction CBCT may have increased the probability of the patient external contour changing (through weight gain or loss). Therefore this time was recorded and the correlation in absolute physical isocentre depth difference (a measure of patient contour change) and absolute isocentre dose difference with time calculated.

3. Results

3.1. Dose comparisons sCT-CT vs sCT-CBCT

The sCT-CBCT isocentre dose differences in Cohort 1 were lower than the sCT-CT differences by -0.7 ± 0.6 % (mean $\pm$95% limits of agreement, see Fig. 2). There were minimal differences between the mean sCT-CT and sCT-CBCT isocentre physical depth differences, 0.2 ± 1.4 mm, suggesting that the CBCT was geometrically similar to the CT. However, there was a substantial difference in mean sCT-CT and sCT-CBCT isocentre radiological depth differences of 2.4 ± 1.7 mm.

The sCT-CBCT gamma pass rates were lower than the sCT-CT pass rates, especially for the 1%/1 mm gamma criteria (see Fig. 4). The mean sCT-CBCT gamma pass rate within the body contour for Cohort 1 was $85 \pm 1\%$ ($\pm$ standard error of the mean, range 75%, 94%), compared to $98.4 \pm 0.2\%$ (95.6%, 99.4%) for the sCT-CT.

3.2. Tolerance levels for sCT-CBCT isocentre dose difference

The mean sCT-CBCT dose difference for Cohort 1 was $\Delta D_{CBCT1} = -0.6 \pm 0.1\%$, ($-1.3\%, 0.6\%$). The 95% confidence interval on the mean was [$-1.5\%, 0.4\%$]. This was rounded to produce asymmetric tolerance levels of [$-2\%, 1\%$]. The mean differences in PTV mean dose, D2 and D98 were $-0.6 \pm 0.1\%, -0.6 \pm 0.1\%$ and $-0.8 \pm 0.1\%$ respectively.

The equivalent results for Cohort 2 were $\Delta D_{CBCT2} = -0.6 \pm 0.1\%$ (-1.3%, 0.6%) for the isocentre dose difference, and $-0.7 \pm 0.1, -0.6 \pm 0.1$ and -0.8 ± 0.1 for the mean differences in PTV mean dose, D2 and D98 respectively. Only 2/29 patients were outside the proposed tolerance levels.

3.3. Evaluation of sCT-CBCT dose differences

The mean sCT-CBCT dose differences across both cohorts was $\Delta D_{CBCT1\&2} = -0.6 \pm 0.1\%$ ($-2.3\%, 2.3\%$). The 95% confidence interval across both cohorts was [$-1.9\%, 0.7\%$] which fitted well with the proposed tolerance levels. The CBCT dose appeared to be systematically lower than the sCT dose, with negative dose differences in 43/49 patients (see Fig. 3).

The gamma analyis showed reasonable agreement between sCT and CBCT with a mean gamma pass rate across both cohorts within the external contour with gamma criteria 1%/1 mm of $86.4 \pm 0.7\%$ (74.5%, 93.6%) and at 2%/2 mm of $96.1 \pm 0.4\%$ (85.4%, 99.7%). The interquartile range of the sCT-CBCT gamma passes overlapped substantially between cohorts 1 and 2 (Fig. 4).

The mean difference in mean radiological isocentre depth was $\Delta d_{Rad} = 1.6 \pm 0.2$ mm (-4.6 mm, 6.1 mm). The mean difference in mean physical isocentre depth was similarly small, $\Delta d_{Phys} = 0.9 \pm 0.2$ mm

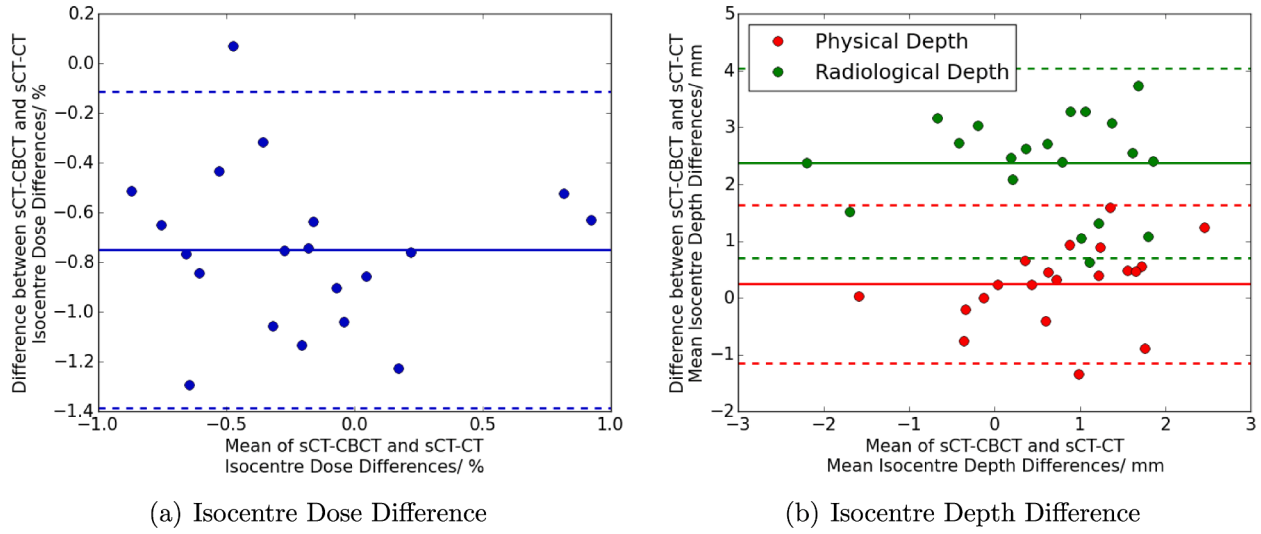

(a) Isocentre Dose Difference (b) Isocentre Depth Difference

Fig. 2. a) Bland–Altman plot of the difference in sCT-CT and sCT-CBCT isocentre dose differences as a function of the mean of the sCT-CT and sCT-CBCT isocentre dose differences. b) Bland–Altman plot comparing mean physical and radiological isocentre depth differences for sCT-CT and sCT-CBCT (red and green respectively). In all plots the circles show the data points, the solid line the mean difference and the dashed line the 95% limits of agreement. Both plots show data from Cohort 1 only.

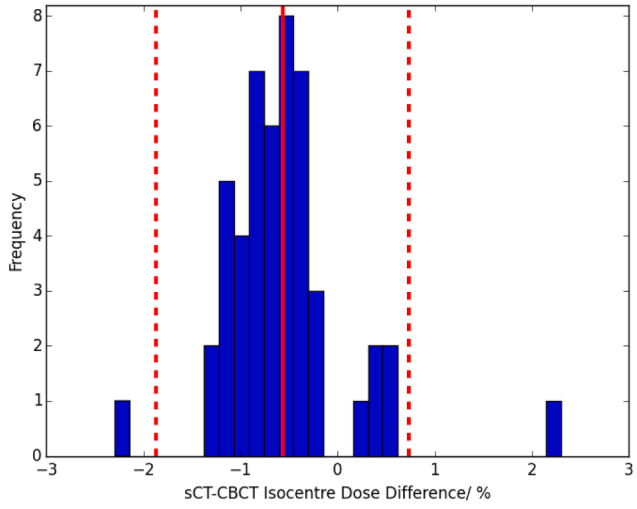

Fig. 3. Histogram of sCT-CBCT isocentre dose differences (CBCT- sCT) for both patient cohorts. The red vertical line indicates the mean, and dashed lines the 95% confidence interval.

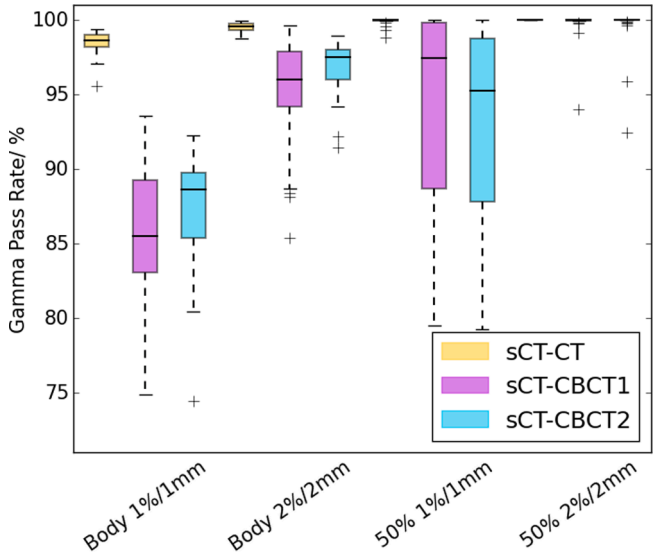

Fig. 4. Boxplot showing gamma pass rates with criteria 1%/1 mm and 2%/2 mm within the external contour (Body) and the volume inclosed by the 50% isodose line (50%) for sCT-CT (yellow), Cohort 1 sCT-CBCT (purple) and Cohort 2 sCT-CBCT (blue). The rectangles indicate the interquartile range (IQR), with the horizontal black line the median value, the black whiskers the maximum (minimum) data point within $Q3 + 1.5IQR$ ($Q1 - 1.5IQR$) and the black crosses outlier data points. One outlier for the 50% isodose line 1%/1 mm results for sCT-CBCT cohort two has been omitted (value 61.5%).

$(-4.3\,\text{mm}, 4.2\,\text{mm})$.

There was a weak correlation between the magnitude of the vector shift between automatic and soft-tissue match and the absolute sCT-CBCT isocentre dose difference, with Pearson's $r = 0.3$ (see Fig. 5). This correlation was approaching statistical significance ($p = 0.06$). There was no statistically significant correlation with absolute mean physical or radiological isocentre depth difference (Pearson's $r = 0.2$, $p = 0.23$ and $r = 0.2, p = 0.18$ respectively). There was no correlation between time from MR to first-fraction and change in physical isocentre depth or isocentre dose difference (Pearson's $r = 0.1, p = 0.51$ and $r = -0.1, p = 0.40$ respectively).

4. Discussion

This study has evaluated using the first-fraction CBCT as a method of dose accuracy QA for a prostate MR-only pathway. Compared to gold standard CT, CBCT has a small but systematic shift in isocentre dose difference of -0.7 %. This was also reflected in a mean sCT-CBCT isocentre dose difference of $\Delta D_{CBCT1\&2} = -0.6 \pm 0.1\%$. There was good agreement in sCT-CBCT gamma pass rates with gamma criteria 2%/2 mm and no correlation between sCT-CBCT isocentre dose difference and the magnitude of soft-tissue match shift or time between MR and first-fraction CBCT.

The sCT-CBCT isocentre dose difference appeared to be systematically lower than the sCT-CT difference, with the 95% limits of agreement not encompassing zero difference (see Fig. 2). This systematic underestimation comes from the difference in radiological isocentre depth (mean difference 2.4 ± 1.7 mm) rather than physical (mean difference

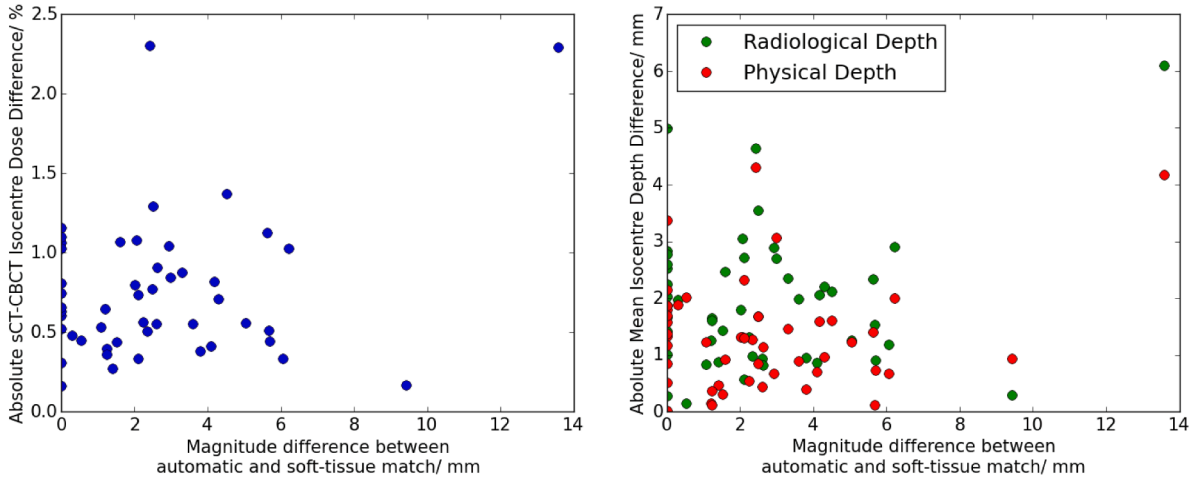

(a) Dose Difference (b) Depth Difference

Fig. 5. The correlation between the magnitude of the vector shift between automatic and soft-tissue match and absolute sCT-CBCT isocentre dose difference (left) and absolute mean sCT-CBCT isocentre depth difference (right) for both cohorts.

0.2 ± 1.4 mm), suggesting it is the CBCT density assignment, rather than the geometrical accuracy, which caused the dose difference. This is consistent with the high geometric accuracy of CBCT, within 1 mm [24]. Dose calculations on CBCT images are known to be less accurate due to the variable photon scatter causing a variable relationship between HU and tissue density [25]. Different methods of dose calculation have been proposed, including applying standard CT, site-specific or patient-specific HU-density curves, bulk density over-rides or deformable registration of a planning CT [25]. Bulk density methods in prostate patients have reported CBCT dose differences to CT of $0.2 \pm 1.3\%$ (mean $\pm$ standard deviation) [19] and 0.4% (median, min 0.0%, max 0.4% [25]. The magnitude of the difference observed in this study was slightly larger but agreed within the 95% limits of agreement ($\pm 0.6\%$).

The lower CBCT dose resulted in worse gamma pass rates than sCT-CT (Fig. 4). The errors in density assignment for the CBCT may also have reduced the gamma pass rates. There was still very good agreement with gamma criteria 2%/2 mm ($96.1 \pm 0.4\%$ within the body contour).

Only one other paper to our knowledge has investigated sCT-CBCT dose differences, reporting mean sCT-CBCT differences in PTV mean dose of $-0.8 \pm 0.6\%$ (CBCT - sCT, $\pm$ standard deviation) [14]. This agrees with the results given here ($-0.64 \pm 0.09\%$ across both cohorts) with the CBCT dose being lower than the sCT dose. They also found the sCT-CBCT dose difference to be larger than the sCT-CT dose difference, although only by 0.3% rather than 0.7% reported here. This may be due to the fact that both CT and CBCT images were calibrated using the same HU to relative electron density curve. This has been reported to improve the mean agreement in dose calculations between CT and CBCT but also increase the standard deviation of differences and the number of outliers [26,25].

The asymmetric 95% confidence interval on the mean sCT-CBCT isocentre dose difference ($[-1.5\%, 0.4\%]$) from Cohort 1 lead to the adoption of asymmetric dose tolerances of $[-2.0\%, 1.0\%]$. Applying these to Cohort 2 resulted in 27/29 patients with isocentre dose differences within these tolerances. The two outlier patients both had substantial changes in the patient external contour (mean physical isocentre depth difference $|\Delta d_{Phys}| > 4$ mm) which were readily observable on the CBCT image, due to weight gain in one instance and different patient posture (clenched buttocks) in the other. This suggests that the CBCT method with tolerances of $[-2.0\%, 1.0\%]$ can accurately detect geometric differences in sCT and CBCT, such as may be caused by geometric distortion in the MR used to generate the sCT. Although in this case both results were false positives, in clinical practice doses differences outside of these tolerances at the start of treatment would be cause for concern and should be investigated, monitored over several fractions and if necessary replanned. This implies that the suggested asymmetric dose tolerance would be appropriate for clinical use.

A potential confounding factor in this study was the use of soft-tissue matching, which means the sCT-CBCT registration used for treatment was not necessarily the optimal registration between the two image sets, but had been modified to ensure that the prostate and seminal vesicles were covered by the PTV. This could have been avoided through the use of a deformable registration between CBCT and sCT to ensure the external contours were identical. However, a deformable registration would mean that the geometry of the CBCT would not have been maintained, removing one of the main rationales for using the CBCT as a QA tool, namely the potential geometric distortion in the MR used to generate the sCT. Alternatively, the original automatic MR-CBCT registration could have been used. This was not used since the only registration matrix stored on the linear accelerator was the treatment position (the soft-tissue match). The radiographers manually recorded the automatic registration position, but to use this position for the sCT-CBCT dose QA process would have required additional manual steps in the process and precluded full automation. The use of soft-tissue matching appears not to have had a substantial impact, with a small correlation (Pearson's $r = 0.3$) between absolute isocentre dose difference and magnitude of the vector shift difference between the automatic and soft-tissue matches. Although this correlation was approaching statistical significance ($p = 0.06$), this was due to the two outlier patients described above. If they are excluded, the correlation disappears (Pearson's $r = 0.0, p = 0.79$). This highlights the dosimetric robustness of MR-CBCT soft-tissue matching and suggests there is only an issue when the patient external contour is substantially different between CBCT and sCT.

Another potential clinical concern for using CBCT for dose accuracy QA for MR-only radiotherapy is that patients may gain or lose weight between planning MR and first-fraction CBCT. This would introduce a confounding dose change, which may be dependent on the length of time between MR and first fraction since longer times would increase the probability of weight change. However, there was no significant correlation in time between physical isocentre depth or isocentre dose difference, suggesting this is not an issue within the period evaluated in this study (maximum 34 days).

A practical consideration of using CBCT for dose accuracy QA for MR-only radiotherapy is the resource implications of recalculating the treatment plan. However, the recalculation process presented here was

highly automated utilising scripts within the treatment planning system and took less than 10 min.

Future work will look to characterise the clinical effectiveness of the method further by determining false positive and false negative rates. This could be through generating deliberate errors such as not applying the 3D distortion correction post-processing to the MR image before generating a sCT and seeing the impact on sCT-CBCT dose differences. Alternatively, retrospective MR images with potential issues (eg significant image artefacts) could be used to generate sCTs and sCT-CT and sCT-CBCT dose differences compared. An investigation procedure for out-of-tolerance results should also be developed and evaluated. This could include visual inspection of the sCT and CBCT, examining the sCT-CBCT registration and the MR used to generate the sCT for potential issues (eg 3D distortion correction applied, appropriate receive bandwidth used, and presence and position of image artefacts). If the out-of-tolerance investigation identifies an issue with the sCT or MR then the patient should be rescanned and replanned.

In conclusion, the first-fraction CBCT appears a promising method for dose accuracy QA of sCT in a MR-only prostate radiotherapy pathway, with a high sCT-CBCT gamma pass rate with 2%/2 mm criteria. There was a small systematic difference in dose between sCT and CBCT, suggesting that asymmetric dose tolerances of $[-2.0\%, 1.0\%]$ would be appropriate clinically. There was no correlation between sCT-CBCT isocentre dose difference and the magnitude of soft-tissue match shift or time between MR and first-fraction CBCT. sCT dose accuracy QA using the first-fraction CBCT would enable departments to safely implement MR-only radiotherapy without the need for back-up CTs.

Declaration of Competing Interest

The authors declare that they have no known competing financial interests or personal relationships that could have appeared to influence the work reported in this paper.

References

[1] Khoo V, Joon D. New developments in MRI for target volume delineation in radiotherapy. Br J Radiol 2006;79:S2–15. https://doi.org/10.1259/bjr/41321492.

[2] Nyholm T, Nyberg M, Karlsson MG, Karlsson M. Systematisation of spatial uncertainties for comparison between a MR and a CT-based radiotherapy workflow for prostate treatments. Radiat Oncol 2009;4. https://doi.org/10.1186/1748-717X-4-54.

[3] Johnstone E, Wyatt JJ, Henry AM, Short SC, Sebag-Montefiore D, Murray L, et al. A systematic review of synthetic Computed Tomography generation methodologies for use in Magnetic Resonance Imaging – only radiation therapy. Int J Radiat Oncol Biol Phys 2018;100:199–217. https://doi.org/10.1016/j.ijrobp.2017.08.043.

[4] Bird D, Henry AM, Sebag-Montefiore D, Buckley DL, Al-Qaisieh B, Speight RA. Systematic Review of the Clinical Implementation of Pelvic Magnetic Resonance Imaging-Only Planning for External Beam Radiation Therapy. Int J Radiat Oncol Biol Phys 2019;105:479–92. https://doi.org/10.1016/j.ijrobp.2019.06.2530.

[5] Tyagi N, Zelefsky MJ, Wibmer A, Zakian K, Bdoieson S, Happersett L, et al. Clinical experience and workflow challenges with magnetic resonance-only radiation therapy simulation and planning for prostate cancer. Phys Imaging Radiat Oncol 2020;16:43–9. https://doi.org/10.1016/j.phro.2020.09.009.

[6] Persson E, Gustafsson C, Nordström F, Sohlin M, Gunnlaugsson A, Petruson K, et al. MR-OPERA-A multi-center/multi-vendor validation of MRI-only prostate treatment planning using synthetic CT images. Int J Radiat Oncol Biol Phys 2017;99:692–700. https://doi.org/10.1016/j.ijrobp.2017.06.006.

[7] Tyagi N, Fontenla S, Zhang J, Cloutier M, Kadbi M, Mechalakos J, et al. Dosimetric and workflow evaluation of first commercial synthetic CT software for clinical use in pelvis. Phys Med Biol 2017;62:2961. https://doi.org/10.1088/1361-6560/aa5452.

[8] Dowling JA, Sun J, Pichler P, Rivest-Hénault D, Ghose S, Richardson H, et al. Automatic substitute computed tomography generation and contouring for magnetic resonance imaging (MRI)-alone external beam radiation therapy from standard MRI sequences. Int J Radiat Oncol Biol Phys 2015;93:1144–53. https://doi.org/10.1016/j.ijrobp.2015.08.045.

[9] Kapanen M, Collan J, Beule A, Seppälä T, Saarilahti K, Tenhunen M. Commissioning of MRI-only based treatment planning procedure for external beam radiotherapy of prostate. Magn Reson Med 2013;70:127–35. https://doi.org/10.1002/mrm.24459.

[10] Walker A, Liney G, Metcalfe P, Holloway L. MRI distortion: considerations for MRI based radiotherapy treatment planning. Australas Phys Eng Sci Med 2014;37:103–13. https://doi.org/10.1007/s13246-014-0252-2.

[11] Torfeh T, Hammoud R, Perkins G, McGarry M, Aouadi S, Celik A, et al. Characterization of 3D geometric distortion of magnetic resonance imaging scanners commissioned for radiation therapy planning. Magn Reson Imaging 2016;34:645–53. https://doi.org/10.1016/j.mri.2016.01.001.

[12] Edmund JM, Nyholm T. A review of substitute CT generation for MRI-only radiation therapy. Radiat Oncol 2017;12:28. https://doi.org/10.1186/s13014-016-0747-y.

[13] Edmund JM, Andreasen D, Mahmood F, Van Leemput K. Cone beam computed tomography guided treatment delivery and planning verification for magnetic resonance imaging only radiotherapy of the brain. Acta Oncol 2015;54:1496–500. https://doi.org/10.3109/0284186X.2015.1062546.

[14] Palmér E, Persson E, Ambolt P, Gustafsson C, Gunnlaugsson A, Olsson LE. Cone beam CT for QA of synthetic CT in MRI only for prostate patients. J Appl Clin Med Phys 2018;19:44–52. https://doi.org/10.1002/acm2.12429.

[15] Wyatt J, Hedley S, Johnstone E, Speight R, Kelly C, Henry A, et al. Evaluating the repeatability and set-up sensitivity of a large field of view distortion phantom and software for magnetic resonance-only radiotherapy. Phys Imaging Radiat Oncol 2018;6:31–8. https://doi.org/10.1016/j.phro.2018.04.005.

[16] Siversson C, Nordström F, Nilsson T, Nyholm T, Jonsson J, Gunnlaugsson A, et al. Technical Note: MRI only prostate radiotherapy planning using the statistical decomposition algorithm. Med Phys 2015;42:6090–7. https://doi.org/10.1118/1.4931417.

[17] Dearnaley D, Syndikus I, Mossop H, Khoo V, Birtle A, Bloomfield D, et al. Conventional versus hypofractionated high-dose intensity-modulated radiotherapy for prostate cancer: 5-year outcomes of the randomised, non-inferiority, phase 3 CHHiP trial. Lancet Oncol 2016;17:1047–60. https://doi.org/10.1016/S1470-2045(16)30102-4.

[18] Wyatt JJ, Brooks RL, Ainslie D, Wilkins E, Raven E, Pilling K, et al. The accuracy of magnetic resonance – cone beam computed tomography soft-tissue matching for prostate radiotherapy. Phys Imaging Radiat Oncol 2019;12:49–55. https://doi.org/10.1016/j.phro.2019.11.005.

[19] Chen S, Le Q, Mutaf Y, Lu W, Nichols EM, Yi BY, et al. Feasibility of CBCT-based dose with a patient-specific stepwise HU-to-density curve to determine time of replanning. J Appl Clin Med Phys 2017;18:64–9. https://doi.org/10.1002/acm2.12127.

[20] Grégoire V, Mackie T, De Neve W, Gospodarowicz M, Purdy J, van Herk M, et al. State of the art on dose prescription, reporting and recording in Intensity-Modulated Radiation Therapy (ICRU report No. 83). Cancer Radiother 2011;15:555–9. https://doi.org/10.1016/j.canrad.2011.04.003.

[21] Nyholm T, Berglund M, Brynolfsson P, Jonsson J. EP-1533: ICE-Studio – an Interactive visual research tool for image analysis. Radiother Oncol 2015;115:S837.

[22] Maspero M, Seevinck P, Schubert G, Hoesl M, van Asselen B, Viergever M, et al. Quantification of confounding factors in MRI-based dose calculations as applied to prostate IMRT. Phys Med Biol 2017;62:948–65. https://doi.org/10.1088/1361-6560/aa4fe7.

[23] Bland JM, Altman D. Statistical methods for assessing agreement between two methods of clinical measurement. Lancet 1986;327:307–10. https://doi.org/10.1016/S0140-6736(86)90837-8.

[24] Kim G, Pawlicki T, Luxton G. SU-FF-I-32: performance and stability of the Varian Cone-Beam CTsystem. Med Phys 2006;33. https://doi.org/10.1118/1.2240271.

[25] Giacometti V, King RB, Agnew CE, Irvine DM, Jain S, Hounsell AR, et al. An evaluation of techniques for dose calculation on cone beam computed tomography. Br J Radiol 2019;92:20180383. https://doi.org/10.1259/bjr.20180383.

[26] Fotina I, Hopfgartner J, Stock M, Steininger T, Lütgendorf-Caucig C, Georg D. Feasibility of CBCT-based dose calculation: comparative analysis of HU adjustment techniques. Radiother Oncol 2012;104:249–56. https://doi.org/10.1016/j.radonc.2012.06.007.